Using Hydrogen as Gas Turbine Fuel

Paolo Chiesa

Giovanni Lozza

Dipartimento di Energetica,
Politecnico di Milano,
Milano, Italy

Luigi Mazzocchi
CESI,
Milano, Italy

This paper addresses the possibility to burn hydrogen in a large size, heavy-duty gas turbine designed to run on natural gas as a possible short-term measure to reduce greenhouse emissions of the power industry. The process used to produce hydrogen is not discussed here: we mainly focus on the behavior of the gas turbine by analyzing the main operational aspects related to switching from natural gas to hydrogen. We will consider the effects of variations of volume flow rate and of thermophysical properties on the matching between turbine and compressor and on the blade cooling of the hot rows of the gas turbine. In the analysis we will take into account that those effects are largely emphasized by the abundant dilution of the fuel by inert gases (steam or nitrogen), necessary to control the NO_x emissions. Three strategies will be considered to adapt the original machine, designed to run on natural gas, to operate properly with diluted hydrogen: variable guide vane (VGV) operations, increased pressure ratio, re-engineered machine. The performance analysis, carried out by a calculation method including a detailed model of the cooled gas turbine expansion, shows that moderate efficiency decays can be predicted with elevated dilution rates (nitrogen is preferable to steam under this point of view). The combined cycle power output substantially increases if not controlled by VGV operations. It represents an opportunity if some moderate re-design is accepted (turbine blade height modifications or high-pressure compressor stages addition).
[DOI: 10.1115/1.1787513]

1 Introduction

Hydrogen, as a carbon-free energy carrier, is likely to play a important role in a world with severe constraints on greenhouse gas emissions. In the power industry, its utilization as gas turbine fuel can be proposed under several possible scenarios, depending on the mode of H_2 production. For instance, hydrogen can be produced remotely from renewable energy sources (solar or wind) or from nuclear energy (via direct thermal conversion or by electrolysis), but in a more realistic and near-term vision it will be derived from conventional fossil fuels by conversion processes including CO_2 sequestration. Possible solutions include: (i) remote coal conversion to hydrogen (via gasification, shift, and separation from CO_2) and H_2 pipeline transport to the power station, (ii) integrated hydrogen and electricity production from coal or natural gas, exporting pure hydrogen to remote users, and using on-site low-grade hydrogen to produce power [1], (iii) electricity generation from combined cycles integrated to fossil fuel decarbonization (applicable to coal, oil, or gas) and to CO_2 capture [2]. Fuel cells and H_2-O_2 semiclosed cycles may represent future options for power generation, but combined cycles coupled to H_2 production/CO_2 sequestration processes can be proposed as a short/mid-term solution for massive greenhouse gas emission reduction.

This paper addresses the possibility to burn hydrogen in a large size, heavy-duty gas turbine designed to run on natural gas, for a prompt application of the above general concepts, regardless of the process used to produce hydrogen and its integrations with the combined cycle. We will focus on the behavior of the gas turbine, by considering the effects of the variation of volume flow rates and of thermophysical properties, related to switching from natural gas to hydrogen. These effects are emphasized by the fact that NO_x emission control relies on fuel dilution with large quantities of inert gases, like steam or nitrogen, as discussed in Sec. 2. The consequent variation of the operating conditions is therefore much larger than for the mere fuel substitution, calling for an analysis of the opportunity (or necessity) of design modifications to the gas turbine. The paper discusses these issues by considering some possible adaptation techniques, by discussing their operational limits and, mostly, by predicting the resulting combined cycle efficiency and power output.

2 NO_x Control

Generally speaking, three methods have been used to reduce NO_x emissions from gas turbine power plants: (i) premixed combustion, including catalytic combustion, (ii) fuel dilution, mostly by steam, water or nitrogen; (iii) removal from exhaust gases. For natural gas applications, the first technique is the preferred one: at present, the ''dry low-emission'' combustors are proposed by manufacturers for virtually any gas turbine model. Their basic principle is to achieve a moderate flame temperature by forcing more air than stoichiometric in the primary zone; this is obtained by mixing air to fuel before the combustion. Catalytic combustors, often referenced as the future technology for extremely low emissions, just enhance the same principle, allowing for a much larger rate of premixing, no longer limited by flame stability limits. When switching to hydrogen (or to hydrogenated fuels, such as the coal syngas used in IGCC plants) premixing becomes a very questionable practice, due to the much larger flammability limits and the lower ignition temperatures of hydrogen with respect to natural gas [3]. Therefore both dry low-emission and catalytic combustors cannot be safely proposed for large industrial applications, to the authors' knowledge, simply because hydrogen promptly reacts when mixed to air at typical gas turbine conditions, at virtually any rate. In fact, IGCC combustors, handling a CO-H_2 mixture with H_2 content from 25 to 40%, are diffusion burners and pre-mixed combustion was never attempted. Massive steam or nitrogen dilution is extensively used in these combustors [4] to control NO_x. In diffusion burners, the stoichiometric flame temperature (SFT) is representative of the actual flame temperature, strictly related to the NO formation rate.

Figure 1 shows a collection of literature data, mostly retrieved from a GE experimental investigation with hydrogenated fuels

Contributed by the International Gas Turbine Institute (IGTI) of THE AMERICAN SOCIETY OF MECHANICAL ENGINEERS for publication in the ASME JOURNAL OF ENGINEERING FOR GAS TURBINES AND POWER. Paper presented at the International Gas Turbine and Aeroengine Congress and Exhibition, Atlanta, GA, June 16–19, 2003, Paper No. 2003-GT-38205. Manuscript received by IGTI October 2002; final revision March 2003. Associate Editor: H. R. Simmons.

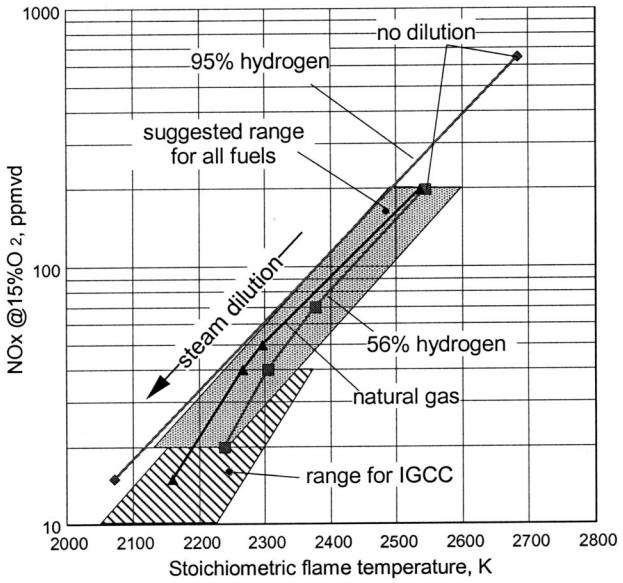

Fig. 1 Relation between NO_x emission and stoichiometric flame temperature, progressively reduced by steam dilution, for gas turbine diffusive combustion at 12–16 bar with different fuels. Nitrogen is the balance gas for 56% and 95% hydrogen.

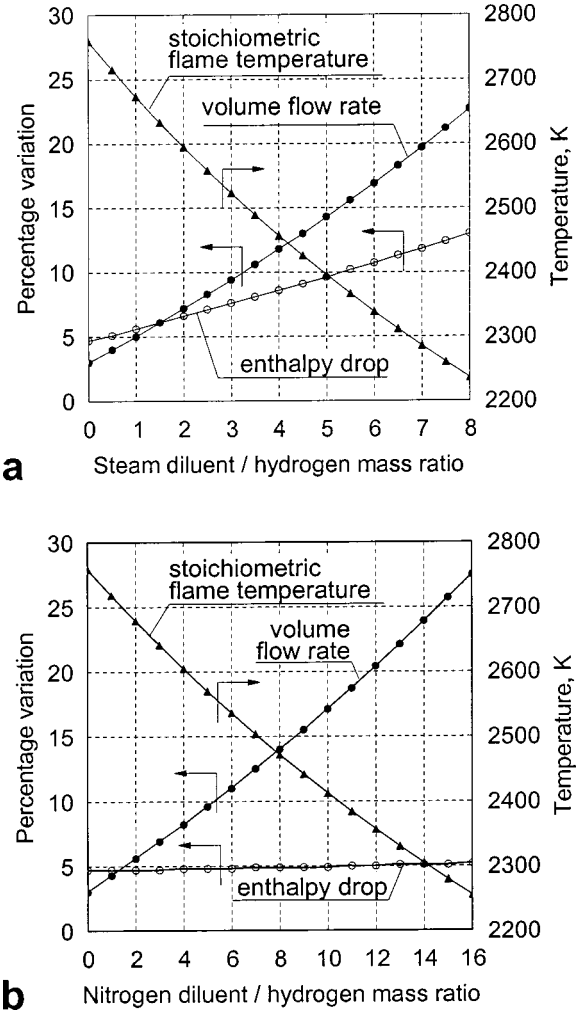

Fig. 2 Variation of the SFT and of the inlet volume flow rate and isentropic enthalpy drop of a hydrogen fueled gas turbine with respect to the reference natural gas case. Curves are drawn as a function of the added diluent flow rate: the upper diagram refers to steam, the lower diagram to nitrogen.

reported by Todd and Battista [5], showing a relation between SFT and NO_x emission for various fuels in typical gas turbine conditions. It is clear that the utilization of undiluted H_2 brings about unacceptable levels of emission and that the SFT must be greatly reduced to have emissions comparable to power industry standards (25–45 ppmvd). A reasonable value of 2300 K for SFT can be stipulated to meet this standards, even if more experience must be gained to set precise indications.

The third technique mentioned above (removal from exhausts) includes: (i) selective catalytic reduction (SCR) by means of ammonia injection (a very well-known method), (ii) the Sconox process, recently proposed for extremely elevated removal rates, using adsorption-desorption on potassium carbonate beds. These techniques can be used downstream of H_2-fueled gas turbines, as well as for conventional units. However, their cost and size are basically related to the amount of NO_x removed (about 2000 $/ton for SCR, 6000–8000 for Sconox (Major and Powers [6])). Their utilization can be proposed to reduce emissions starting from a moderate concentration (for instance from 100 to 10 ppm), but the incidence on the electricity cost would be excessive when starting from many hundreds of ppm, as for H_2 combustion (especially for Sconox). Therefore, excluding premixed combustors and limiting the SCR to ''finishing'' applications, dilution techniques seem mandatory for hydrogen utilization in gas turbine combustors.

The selection of steam and nitrogen as the possible diluents is quite straightforward. Steam is always available in a combined cycle and can be extracted from the steam turbine at any pressure and at any reasonable rate. Nitrogen is available ''for free'' in processes including air separation, i.e., in any coal or refinery residual gasification plant: if the hydrogen used by the gas turbine is produced on site from decarbonization of syngas from heavy fuels, nitrogen will be surely present in large quantities[1] (see, for instance, Lozza and Chiesa [2]). In such plants, it is also possible to use saturation of the hydrogen-rich gas by means of warm water coming from the syngas cooling: it makes available a steam-diluted fuel without extractions from the steam turbine. In some other hydrogen production processes, nitrogen is ''naturally'' available: this is the case of natural gas decarbonization by means of an air-blown autothermal reformer [7,8], producing a synthesis fuel consisting of a 50–50% (approximately, by volume) mixture of H_2 and N_2, perfectly suited for NO_x abatement.

[1]Throughout the discussion we will assume that nitrogen for dilution is available at no energy cost at atmospheric pressure. This assumption is actually verified if the plant incorporates a low-pressure air separation unit.

3 Effects of Hydrogen Combustion on Turbomachinery

Compared to natural gas, hydrogen combustion leads to a lower mass flow rate and to a different composition of the product gases, with an higher water content that in turn influences the molecular weight and the specific heat of the mixture. The most relevant effects on the operation of a gas turbine are: (i) a variation of the enthalpy drop in the expansion, (ii) a variation of the flow rate at the turbine inlet which, in turn, affects the turbine/compressor matching, (iii) a variation of the heat-transfer coefficient on the outer side of the turbine blades, affecting the cooling system performance.

3.1 Influence of Fluid Composition Variation on Turbine Enthalpy Drop and Inlet Volume Flow Rate. Figure 2(*a*) shows the influence of hydrogen combustion (in presence of a variable flow of diluting steam) on the isentropic enthalpy drop of a turbine at a given inlet condition ($T=1450°C$, $p=17$ bar) and

atmospheric outlet pressure, compared to the corresponding natural gas fired case. Compared to natural gas, the simple hydrogen combustion increases the enthalpy drop by about 5%, a variation that increases as long as the amount of added steam rises. Assuming the working fluid as an ideal gas, since the isentropic enthalpy drop can be evaluated through the expression

$$\Delta h_{is} = \int_{T_{FIN,IS}}^{T_{IN}} c_P(T)dT = \overline{c_P}(T_{IN} - T_{FIN,IS}),$$

it is possible to distinguish the effect due to the variation of average c_P and the one due to the variation of the temperature drop through the expansion (being the latter influenced by the exponent of the isentropic transformation γ, i.e., the specific-heat ratio). Increasing steam dilution entails an enhancement of the mixture specific heat but a simultaneous decrease of the exponent γ that reduces the temperature drop and consequently increases the turbine outlet temperature.

The second *y* axis reports the stoichiometric flame temperature resulting from the combustion. It shows that a diluent to H_2 mass ratio of about 7 is required to keep this temperature at 2300 K: correspondingly the enthalpy drop increases by about 12% with respect to the natural gas case.

Figure 2(*a*) also quantifies the variation of the volume flow rate at turbine inlet resulting from the hydrogen combustion (always in comparison with the natural gas fired case). The same amount of combustion air and the same combustion temperature (1450°C) are assumed for all the cases and therefore also the H_2 flow rate increases as long as the diluent flow rate increases. Notice that in the case of no dilution, although the mass flow rate of combustion products reduces (about 2%, considered that hydrogen LHV is 119.95 MJ/kg versus 44.77 of natural gas), the volume flow rate increases by about 3% due to the change in composition (molecular weight of this mixture reduces from 28.27 to 26.93 kg/kmol). This effect amplifies when dilution is considered. At steam to H_2 mass ratio of 7 the mass and volume flow rate increase by 11% and 20%, respectively.

Figure 2(*b*) reports the analysis as far as nitrogen is considered for dilution. The different scale on the abscissa reflects that a much larger diluent to fuel ratio is required to determine a given SFT abatement (about twice, since c_P of N_2 is approximately one-half of c_P of steam). Therefore dilution greatly affects the mass flow rate and, consequently, the volume flow rate (black dotted line). On the contrary the effect of nitrogen dilution on the turbine enthalpy drop is virtually negligible since a large amount of nitrogen (from combustion air) is already contained in the mixture so that even a large diluent addition does not substantially modify the fluid properties.

3.2 Compressor/Turbine Matching. Because of the variation of the volume flow rate caused by the different fuel (and additional diluent), using hydrogen affects the original matching between compressor and expander in a gas turbine originally designed to run on natural gas. A different running point will be set where mass flow rate and pressure ratio will restore the fluid-dynamic equilibrium between the two turbomachines. Typical operational curves are shown in Figs. 3 and 4, for a single shaft arrangement operating at fixed rotational speed (the only solution adopted for large industrial gas turbines). For high performance axial compressors with several transonic stages, used in advanced gas turbines, the characteristics show that the mass flow rate is virtually constant when the inlet is choked. To improve partial load operations, variable geometry guide vanes (VGV's) are used on several stator rows, affecting the characteristic lines as shown by Fig. 3.

The operating line of the expander at constant speed is reported in Fig. 4. When the machine is fueled with hydrogen, having a higher heating value than natural gas, the mass flow rate $G_{T,IN}$ reduces for a give compressor airflow. Nevertheless the nondimensional flow $G_{R,T,IN}$ slightly increases, because of the molecular mass reduction. This increase becomes more and more important when $G_{T,IN}$ grows up due to the diluent addition. Therefore switching from natural gas to hydrogen makes impossible to operate the gas turbine on the same running point (i.e., at the same VGV angle, pressure ratio, $G_{C,IN}$ and $T_{T,IN}$).

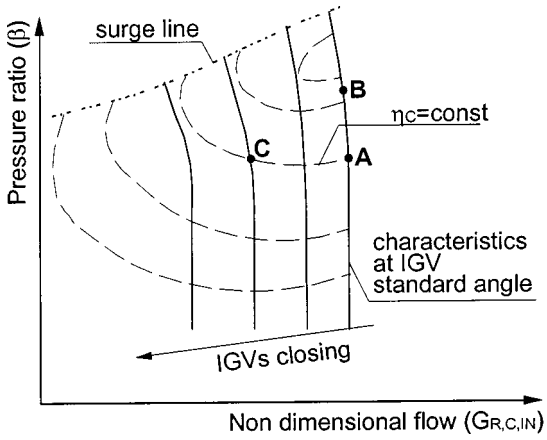

Fig. 3 Typical compressor characteristic curve at constant rotational speed. Different lines correspond to different settings of the variable guide vanes angle.

Assuming that A and A' are the design points on the compressor and turbine maps (Figs. 3 and 4) of the natural gas fueled machine, three different regulation strategies can be envisaged:

(i) Letting the compressor to work at the same point (*A*, at the same VGV angle) and reducing the $T_{T,IN}$, to restore the fluid-dynamic matching between compressor and turbine. The expander runs at the design point A':

(ii) Letting the VGV angle and $T_{T,IN}$ at their original value, $G_{R,T,IN}$ can be adjusted by increasing the pressure ratio, (i.e. moving from A to B on the compressor characteristics while the turbine running point moves from A' to B'). If the compressor is not choked, the higher β also reduces the mass flow rate and helps to reset the matching. If the required pressure ratio exceeds the available surge margin, one or more high-pressure stages must be added to the compressor.

(iii) Letting $T_{T,IN}$ and β at their value, equilibrium can be found by closing the VGV's and reducing $G_{C,IN}$. The corresponding running point moves from A to C in Fig. 3. If condition depicted by point C exceeds the available surge margin, additional stages are required. The turbine running point remains unaffected so that C' overlaps A'.

Remarking that the actual regulation can be carried out by adopting all the three strategies at the same time, it is evident that the first one seems the least interesting since the performance of a combined cycle substantially decays when $T_{T,IN}$ reduces. The effects of the latter strategies on the cycle performance will be dis-

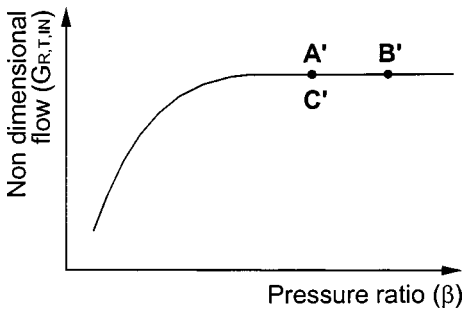

Fig. 4 Typical turbine characteristic curve at constant rotational speed

Table 1 Thermophysical properties at 1000°C and 10 bars

	ρ, kg/m^3	c_P, kJ/kg K	$\mu\times10^6$, Pa s	k$\times10^3$, W/m K	$\rho^{0.63}c_P^{1/3}k^{2/3}/\mu^{0.7}$
Air	2.736	1.183	50.109	83.164	73.84
Steam	1.702	2.482	48.241	135.465	98.15
CO_2	4.158	1.289	49.524	81.696	98.09

cussed later (Sec. 5), but it can be anticipated that off-design operations imply a substantial change of the gas turbine power output. Therefore considerations about mechanical stresses can heavily influence the regulation strategy: dealing with such limits is beyond the scope of the present analysis but they must be carefully considered.

The hydrogen combustion (and related dilution) also entails substantial changes in the shape of the velocity triangles, due to the increase of the enthalpy drop and volume flow rate that influence the flow velocity and its axial component, respectively. Given that the flow is accelerated along the gas path, the turbine blades can operate efficiently even for incidence angles sensibly different from the design value and these changes in the velocity triangles consequently have small effects on the turbine performance. A more relevant efficiency decay can be caused by the increase of the kinetic energy loss at the exhaust due to the increased flow rate for the same exhaust area.

3.3 Blade Cooling. Hydrogen combustion and additional dilution affect the cooling system under two different aspects:

• the varied composition of the hot stream enhances the convective heat-transfer coefficient on the outer side of the blade increasing the thermal flux with negative consequences on the performance of the cooling circuit;

• the higher pressure ratio increases the convective heat-transfer coefficients on both blade sides and the temperature of air used in the cooling circuit whose performance decays.

Effect of Flow Composition. The correlation proposed by Louis [9] allows us to evaluate the average heat-transfer coefficient on the outer side of the blade:

$$h_{\mathrm{OUT}}=0.285\frac{(\rho v)^{0.63}c_P^{1/3}k^{2/3}}{D^{0.37}\mu^{0.7}},$$

where v is the main stream speed referred to the cascade exit. Replacing steam to CO_2 (as it actually occurs when H_2 replaces natural gas as fuel) has no significant consequences on the heat flux imposed on the blade outer surface, as it can be argued from Table 1. On the contrary, steam dilution determines an increase of the thermal flux since the heat-transfer coefficient for steam is higher than for air. A secondary effect is an increase of h_{OUT} due to the higher average velocity of the gas stream along the flow path related to the higher available enthalpy drop.

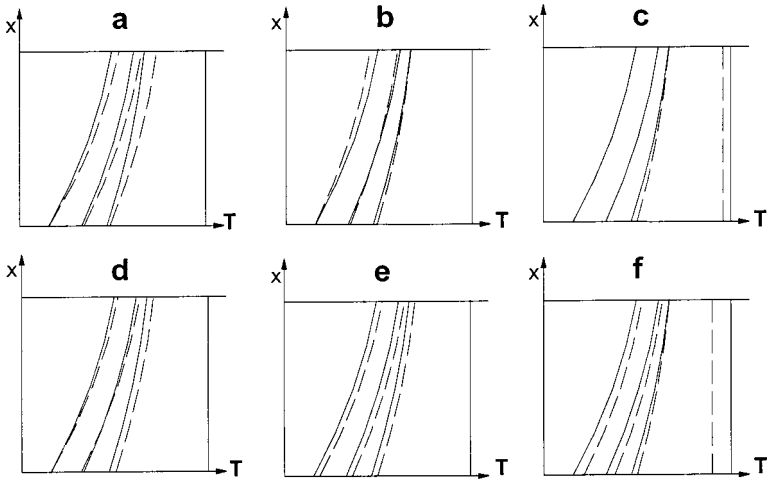

Fig. 6 Temperature–heat-transfer area diagrams showing different situations in the simplified cooling circuit of Fig. 5. Temperature profiles have the same meaning of Fig. 5: from left, they refer to coolant, inner blade wall, outer blade wall, main gas stream. The continuous lines refer to the original situation, the dashed ones to modified conditions.

Although the calculation model used for the final discussion (Sec. 5) considers the current gas turbine cooling circuits including film cooling and multipass channels, the behavior of a cooling circuit in consequence of a change in the main stream composition can be better discussed by considering a very simplified convective cooling circuit. It consists of a single internal duct run by the cooling fluid whose blade transverse section is schematically shown on the left side of Fig. 5. The temperature profiles along the blade height are shown in Fig. 5, right side. The blade can be considered a cross-flow heat exchanger, where the cooling flow ensures that the highest metal temperature remains within the stipulated limit.

Enhancing the thermal flux on the blade at constant cooling flow rate causes an increase of the temperatures along the profiles as shown in Fig. 6(*a*). The constraint on the maximum metal temperature can be restored either by increasing the cooling flow

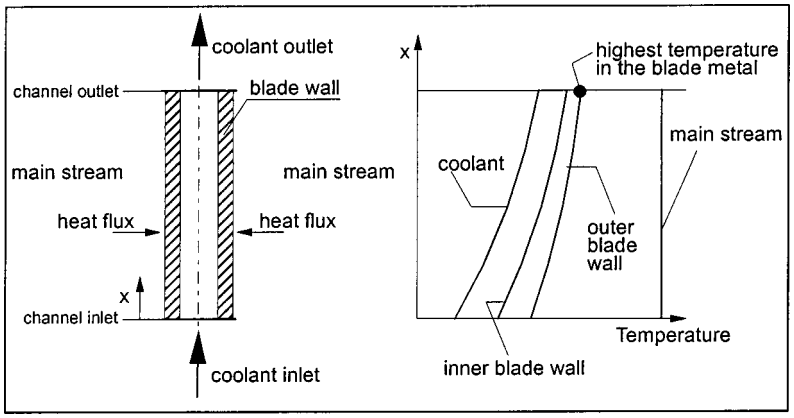

Fig. 5 Simplified blade cooling model. Blade is assumed as a cross-flow heat exchanger where heat capacity of the outer stream is infinitely larger than the one of the inner stream. Main temperature profiles are reported in the right diagram.

rate (Fig. 6(*b*)) or by reducing the temperature of the outer stream (Fig. 6(*c*)). In hydrogen operation of a gas turbine designed to run on natural gas, it seems straightforward that the cooling circuit does not change and therefore the solution of Fig. 6(*b*) cannot be adopted. Decreasing the turbine inlet temperature (Fig. 6(*c*)) appears the only feasible alternative.[2]

Effect of Pressure Ratio. An increase of the cycle pressure ratio influences the blade cooling mechanisms in three main aspects: (i) the heat-transfer coefficients enhance on both the inner and the outer blade side due to the fluid density increase; (ii) the temperature of the cooling air from compressor increases; (iii) the coolant mass flow rate increases because of coolant density increase for a given circuit geometry. About the first point, we already discussed the negative effects of an h_{OUT} enhancement. On the contrary, an enhancement of h_{COOL} has positive effects because it reduces the temperature difference between the fluid and the metal blade. Nevertheless, the simultaneous and proportional enhancement of the heat-transfer coefficient on both the blade sides due to the pressure ratio increase is not neutral because it increases the heat flux (and consequently the temperature drop) across the blade wall, bringing the maximum metal temperature beyond its admissible value (Fig. 6(*d*)). Finally, a coolant temperature increase causes the shift of all the temperature profiles as shown in Fig. 6(*e*). A temperature decrease of the flow at the turbine inlet is then required to restore the capability of the cooling circuit to meet the imposed limits (Fig. 6(*f*)) although this effect is somehow mitigated by the coolant flow increase allowed by the higher β.

4 Calculation Methodology

The performance prediction was carried out by a computer code developed by the authors' research group during several years of activities about gas turbine power plants. For a comprehensive description, see Chiesa and Macchi [10]. As a brief reminder, the main features of the code include the capability of reproducing very complex plant schemes by assembling basic modules (such as turbine, compressor, combustor, steam section, heat exchanger, etc.) and an effective prediction of the efficiency of turbomachines (gas and steam turbine stages, compressors) at their design point by means of built-in correlations. The calculation process also includes the one-dimensional design of the gas turbine stages, useful to establish all the aerodynamic, thermodynamic, and geometric characteristics of each blade row necessary for an accurate estimation of the cooling flows and the evolution of the cooled expansion. The cooling model accounts for film cooling, thermal coatings, and multipassage internal channels with enhanced heat-transfer surfaces. These effects are evaluated by means of some parameters, calibrated to reproduce the performance of advanced gas turbines. The complete procedure is reported in Ref. [10].

Even if the code is conceived for prediction of gas turbine performance at the design point only, introduction of convenient hypotheses on off-design behavior of turbomachines has made possible calculating the performance of hydrogen fueled combined cycles. We suppose that off-design operations are limited to the gas turbine because of the extreme rigidity of its design. Heat recovery steam generator and steam turbine can be easily adapted to run at the different conditions resulting from H_2 combustion, due to a more flexible manufacturing.

The ''reference'' natural gas combined cycle was calculated by using a set of assumptions reported by Table 2. The main data for the gas turbine are tuned to describe a Siemens V94.3A unit, representative of a state-of-the-art, heavy-duty, single-shaft machine [11]. The assumptions for the steam cycle calculation reproduce the present technological standards. The efficiency (38.17 and 57.57%) predicted for the gas turbine and the combined cycle, respectively, are in good agreement with declared data (38.20 and 57.30%). The same holds for power output (259.4 and 387.2 MW versus 260 and 390 MW). The assumptions of Table 2 were used for all the cases considered, apart from the gas turbine air flow, pressure ratio, and TIT, varied according to the following discussion. In fact, according to Sec. 3, different approaches can be adopted to use hydrogen as the fuel; three alternatives will be considered in the paper:

[2]The rationale underlying this strategy is that the same lifetime of a machine running on natural gas can be preserved in hydrogen operations by maintaining the same maximum metal temperature.

Table 2 Main assumptions for reference cycle calculations

Gas turbine	
	Ambient condition: 15°C, 1.0132 bar, 60% RH
	Inlet/outlet pressure losses=1/3 kPa
	Air/exhaust gas flow=633.8/644 kg/s
	Pressure ratio=17, TIT=1350°C
	Natural gas LHV=44.769 MJ/kg, preheated at 185°C
Steam cycle (three pressure levels, reheat)	
	Evaporation pressures: 166/36/4 bar
	Condensing pressure: 0.0406 bar
	Maximum steam temperature at SH/RH outlet=565°C
	ΔT at pinch point=8°C, at SH approach point=25°C
	Auxiliaries consumption=1% of heat rejected

VGV Operation. In this case no major modifications are required to the gas turbine provided that the stall margin is guaranteed. Additional high-pressure compressor stages can help to recover this margin. Calculation proceeds keeping the pressure ratio at the design value, with an inlet airflow reduced to recover the matching between compressor and turbine. Given the shape of efficiency curves on the compressor map (Fig. 3), it has been assumed to keep the compressor efficiency at the design value (the actual variation of efficiency depends on specific design criteria and cannot be generalized). The turbine maintains the original geometry (diameters, blade heights, angles) and cooling circuit characteristics but runs on a lower TIT in order to maintain the same blade metal temperature of the natural gas case. The different enthalpy drop is accommodated by varying the load on each stage at constant degree of reaction: according to Sec. 3, effects of loading on the stage efficiency have been neglected, but variations of the kinetic energy at the turbine outlet were kept into account.

Increased β. The second approach assumes that the VGV's remain full open and compressor/turbine matching is reset by increasing the operating pressure ratio. Calculation proceeds by assuming that the compressor characteristics is vertical (constant airflow). Given the stall margins available on the actual machines, it is really doubtful that this strategy can be adopted without any modification to the machine design, especially when SFT of 2300 K are demanded. Probably, one or more high-pressure compressor stages must be added [12,13] shifting upward the surge limit. In this case every compressor stage operates very close to the design point so that their efficiency can be correctly predicted by the code built-in correlations. Assumptions for turbine calculation are the same used in the previous case. TIT experiences a more significant decrease, justified by the warmer cooling flows and the higher heat-transfer coefficients related to the higher β.

Re-engineered Machine. In this case the standard machine is re-designed to comply with the larger flow rate at the turbine inlet. The compressor is virtually unchanged and the turbine blade height is increased to accommodate the larger gas flow. In this approach, turbine geometry and blade cooling flows are adapted to operate the gas turbine at the same β and TIT of the standard machine. Since the calculation is based on the very same assumptions used for the natural gas fired machine, this case represents the highest performance limit attainable with a hydrogen fueled gas turbine of the assigned technology level.

Table 3 Main results of the investigation (GT: gas turbine, SC: steam cycle)

Fuel	Nat. gas	Hydrogen, VGV operation			Hydrogen, increased β			Hydrogen, re-engineered		
Diluent	none	none	steam	nitrogen	none	steam	nitrogen	none	steam	nitrogen
Dil./fuel mass ratio	0.00	0.00	6.78	14.44	0.00	6.92	15.36	0.00	6.83	14.45
SFT, K	2545	2745	2300	2300	2746	2300	2300	2745	2300	2300
Pressure ratio	17.00	17.00	17.00	17.00	17.05	18.47	19.73	17.00	17.00	17.00
TIT, °C	1350	1339	1316	1340	1339	1305	1319	1350	1350	1350
TOT, °C	585.1	574.7	577.2	574.2	574.1	562.7	548.6	584.0	591.4	569.5
Air flow, kg/s	633.8	631.9	584.1	550.7	633.8	633.8	633.8	633.8	633.8	633.8
Gas flow, kg/s	644.0	632.7	623.5	631.1	634.6	676.5	728.2	634.7	678.1	725.9
Fuel flow, kg/s	15.02	5.58	5.67	5.52	5.59	6.02	6.11	5.66	6.31	6.31
Diluent flow, kg/s	0.00	0.00	38.44	79.67	0.00	41.71	93.78	0.00	43.10	91.21
Ma_{AX}	0.441	0.437	0.442	0.437	0.439	0.479	0.504	0.441	0.441	0.441
Cooling flows, kg/s	139.8	138.0	138.4	138.1	138.3	146.2	149.0	143.6	168.9	163.1
GT output, MW	256.8	264.5	292.0	297.6	265.1	314.4	340.5	266.3	323.8	342.7
SC net output, MW	130.4	125.6	91.5	125.3	125.7	92.1	132.4	130.1	104.9	142.1
N_2 compressor, MW	0.0	0.0	0.0	42.7	0.0	0.0	54.3	0.0	0.0	48.9
Total output, MW	387.2	390.1	383.5	380.2	390.9	406.4	418.6	396.4	428.7	436.0
LHV efficiency, %	57.57	58.32	56.38	57.46	58.32	56.25	57.15	58.35	56.60	57.57

5 Discussion of Results

The general results of the investigation are reported in Table 3, showing details of (i) the reference natural gas cycle, (ii) the three pure hydrogen fueled cases, calculated according to the strategies described in Sec. 4, (iii) the three hydrogen cases with steam dilution to achieve 2300-K SFT, (iv) the same cases repeated for nitrogen dilution. Figures 7(*a*)–(*f*) reports the most relevant parameters of the calculated cycles as a function of the SFT, i.e., by varying the hydrogen dilution rate.

5.1 Results With VGV Operations (Constant β). As discussed in Sec. 3, pure hydrogen combustion products show superior heat-transfer capabilities and a lower TIT must be selected (11 K—see Table 3). To keep the same pressure ratio, the airflow remains almost unchanged, as well as the heat input (LHV), for a number of reasons related to the variations of molecular mass, inlet temperature, nozzle cooling flow. The gas turbine power increases (3%), due to a larger turbine enthalpy drop, but the steam cycle loses some power (5 MW), due to a lower TOT (about 8 K) and gas flow. The total power slightly increases (0.7%) and a better efficiency is predicted. Note that this efficiency increase is not related to any improvement in the power cycle. It just depends on the thermodynamic properties and on the different lower heating value of the fuels (in fact, the higher heating value reduces efficiency).

When using steam dilution, we obtain (with respect to the undiluted H_2 case) (i) a lower TIT (Fig. 7(*c*), i.e., 23 K at dilution for SFT=2300 K), due to the higher heat-transfer capabilities of hot gases with larger water content, (ii) a reduced air flow (Fig. 7(*d*)), to accommodate for the added diluent flow, (iii) a relevant improvement of the gas turbine output (lower compressor power due to lower air flow, elevated turbine power due to a larger enthalpy drop), (iv) a reduced steam turbine output, due to the steam extraction. Therefore the total output does not change dramatically (Fig. 7(*a*)) but a different gas to steam turbine power ratio can be depicted (Fig. 7(*f*)). A loss of efficiency is predicted (Fig. 7(*b*): 2 percentage points at elevated dilution), because of the detrimental effects of steam/air mixing (typical of mixed gas/steam cycles, as discussed by Macchi et al. [14]).

The situation is different with nitrogen dilution, because: (i) the TIT and the TOT do not change significantly, the gas properties being very little affected by N_2 addition, (ii) the compressor air flow must be reduced because of nitrogen injection, to keep the $G_{R,T,IN}$ unchanged, (iii) the gas turbine power increases due to the lower compression power, (iv) the steam turbine power remains unchanged (same TOT and gas flow), (v) the N_2 compressor power requirement is larger than the power augmentation of the gas turbine (42.7 MW versus 33 for the cases reported in Table 3), because it is less efficient than the gas turbine compressor (85.0% versus 92.4 on a polytropic basis) and brings the nitrogen (from atmospheric pressure) to a larger pressure than combustion air (1.2 times), sufficient for fuel mixing. Therefore the power output and the efficiency reduce with N_2 injection, mostly due to the above quoted effects regarding N_2 compression: the cycle thermodynamics is practically unmodified (differently from steam injection, strongly affecting the cycle with larger efficiency losses).

5.2 Results at Increased β (Constant Air Flow). When using pure hydrogen as the fuel, results are very similar to the previous case (a negligible variation of β here, of airflow there). On the contrary, significant differences arise with large dilution ratios: a larger pressure ratio is required to accommodate for the larger gas flow at the same airflow and turbine nozzle area. TIT must be reduced to keep into account for the higher coolant temperature (a consequence of the larger β), in addition to different heat-transfer properties of steam-rich mixtures. Figure 7(*e*) and Table 3 show that β must be increased to 18.5 for steam and to 19.7 for N_2 if the SFT should be kept at 2300 K, requiring the addition of at least one compressor stage. Compared to VGV operations, the TIT reduction is much larger (Fig. 7(*c*)) because of the higher coolant temperature (436°C at β=19.7 versus 406 at β=17), even if slightly larger cooling flow rates result from increased β, assuming that coolant passages are unmodified.

The lower TIT is the main reason for the lower efficiency obtained for the present cases (Fig. 7(*b*)); another reason is the increased kinetic energy loss at the turbine exhaust because of the higher flow rate through the same annulus area. The power output (Fig. 7(*a*)) is much higher than for the cases with VGV operations, because the air flow rate is no longer reduced and full advantage is taken from the added diluent flow. For the 2300-K dilution the gas turbine power rises to 314 MW (steam) and 340 MW (N_2) from an original value of 257 MW. Such a large modification will require a number of mechanical adaptations and a larger generator in addition to a modified compressor. Similar situations were encountered in the development of gas turbines for IGCC applications [12,13].

5.3 Results for the Re-engineered Machine. This is the situation showing the minimum impact on the cycle efficiency and the maximum improvement of the power output. With respect to the previous case, a larger power output is accomplished because a TIT reduction is no longer necessary, due to the same coolant temperature (unmodified pressure ratio) and to the adaptation of the cooling circuit to the different heat transfer capabilities (Table 3 shows that cooling flows vary according to the turbine flow, determining the blade surface). On another side, keeping the design pressure ratio allows for the optimum cycle configurations:

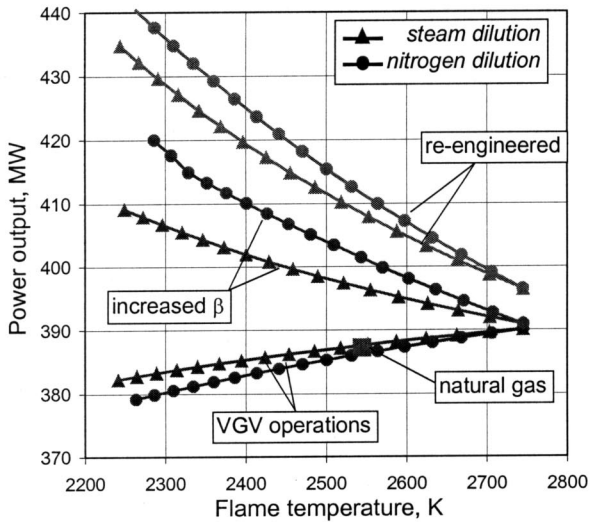

Fig.7a: Combined cycle net power output

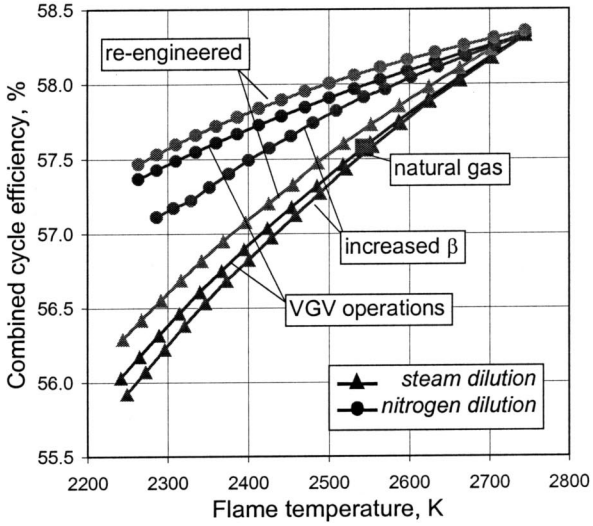

Fig.7b: Combined cycle net efficiency

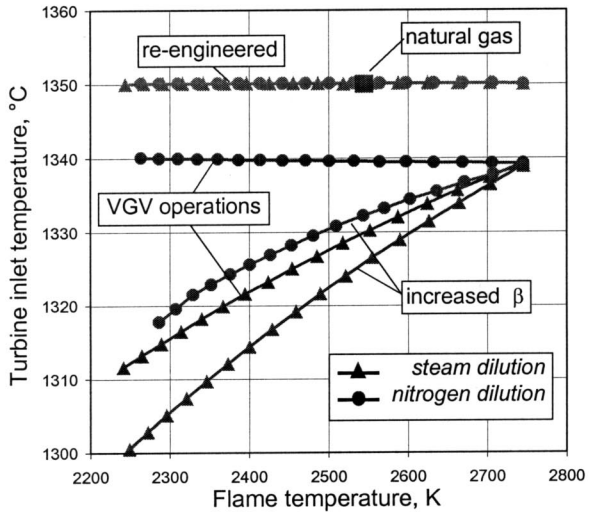

Fig.7c: Total temperature at first rotor inlet (TIT)

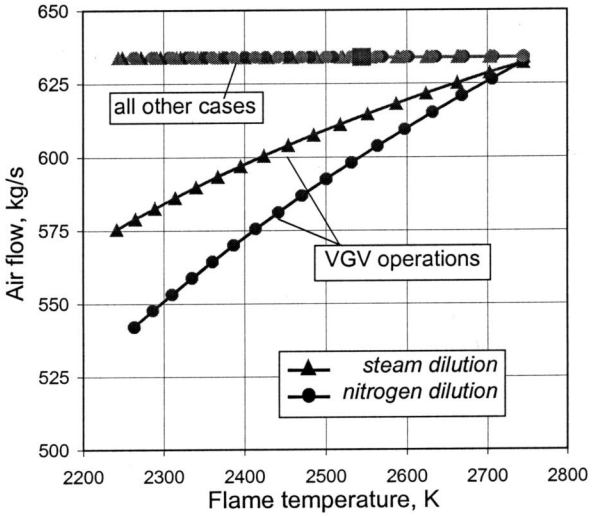

Fig.7d: Air flow at compressor inlet

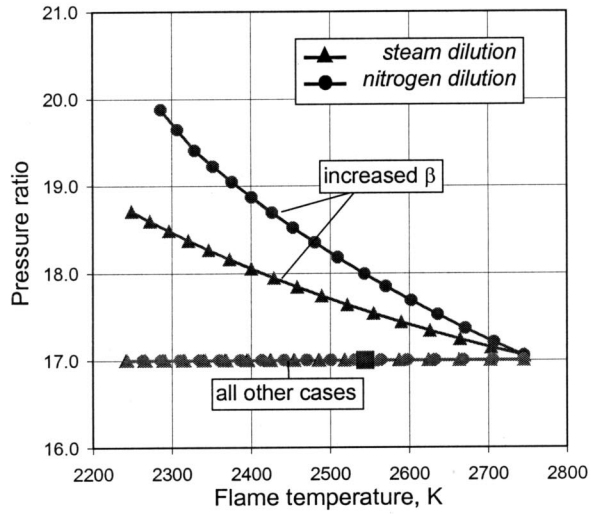

Fig.7e: Gas turbine pressure ratio

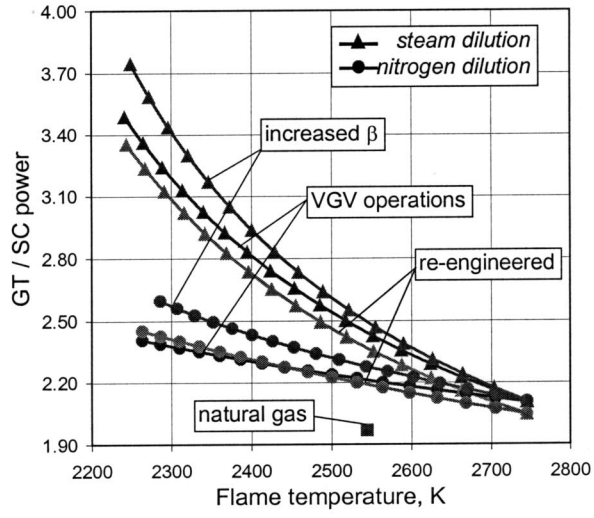

Fig.7f: Gas turbine / steam cycle power output

Fig. 7 (*a*) Combined cycle net power output, (*b*) combined cycle net efficiency, (*c*) total temperature at first rotor inlet (TIT), (*d*) air flow at compressor inlet, (*e*) gas turbine pressure ratio, (*f*) gas turbine/steam cycle power output

the efficiency decays for the same reasons described for VGV operations (steam mixing or higher pressure of compressed N_2, depending on the diluent).

6 Conclusions

The simulations carried out in this work allow a positive answer to the issues related to hydrogen combustion in modern gas turbines. However, a SFT abatement to about 2300 K seems necessary to comply with NO_x emission limits without incurring excessive operating costs of the end-of-pipe de-nitrification systems. This is possible without dramatic performance losses by means of a massive fuel dilution with steam or nitrogen (the latter providing minor losses of efficiency). Different strategies have been envisaged to operate the gas turbine in presence of dilution. Looking at the VGV operated solution (which appears the most likely for the first realizations) the efficiency loss is limited to 0.9 points for nitrogen dilution and 1.9 for steam dilution. Equally small is the influence on the combined cycle power output provided that the gas turbine power output can be increased (by about 10%) in consequence of the compressor airflow reduction. The other solutions here investigated (increased pressure ratio and re-engineered machine) are not particularly attractive in terms of efficiency but provide a much larger power output, an opportunity to reduce the specific costs provided that engineering costs are divided upon a sufficient number of units. It must also be noticed that VGV operations reduce the part-load capabilities of the machine, but make the gas turbine rather insensitive to elevated ambient temperatures (the ''natural'' power loss can be compensated by re-opening the VGV's). As a final consideration on system costs, it can be said that steam dilution allows for reduced capital cost compared to nitrogen, even if providing lower efficiency. In fact, a smaller steam turbine and condenser can be adopted, while the N_2 dilution requires a bulky and expensive additional compressor.

Acknowledgment

The work has been performed within the research on the Italian Electrical System ''Ricerca di Sistema'' Ministerial Decrees of January 26, 2000, and April 17, 2001.

Nomenclature and Acronyms

c_P = specific heat at constant pressure, J/kg K
D = reference blade dimension (chord), m
G = mass flow rate, kg/s
G_R = nondimensional mass flow rate ($G\sqrt{RT}/p$)
h = heat transfer coefficient, W/m^2 K
k = thermal conductivity, W/m K
LHV = lower heating value, MJ/kg
Ma_{AX} = axial Mach number at turbine outlet
p = pressure, Pa
SFT = stoichiometric flame temperature, K
T = temperature, °C or K
TIT = first rotor total inlet temperature, °C
TOT = turbine outlet temperature, °C
v = flow velocity, m/s
VGV = variable guide vanes
β = compressor pressure ratio
Δh = enthalpy drop, J/kg
γ = specific heat ratio
η = efficiency
μ = dynamic viscosity, Pa s
ρ = density of the gas stream, kg/m^3

Subscripts

C = relative to the compressor
COOL = coolant side of the blade wall
FIN = final condition
IN = inlet condition
IS = isentropic
OUT = outer side of the blade wall
T = relative to the turbine

References

[1] Kreutz, T. G. et al., 2002, ''Production of Hydrogen and Electricity From Coal With CO_2 Capture,'' *Proc. of the Sixth International Conference on "Greenhouse Gas Control Technologies"*, Kyoto, Japan.
[2] Lozza, G., and Chiesa, P., 2002, ''CO_2 Sequestration Techniques for IGCC and Natural Gas Power Plants: A Comparative Estimation of Their Thermodynamic and Economic Performance,'' *Proc. of the Int'l Conference on Clean Coal Technologies (CCT2002)*, Chia Laguna, Italy.
[3] Drell, I. L., and Belles, F. E., 1957, ''Survey of Hydrogen Combustion Properties,'' NACA Report 1383, Research Memorandum E57D24.
[4] Huth, H., Heilos, A., Gaio, G., and Karg, J., ''Operation Experiences of Siemens IGCC Gas Turbines Using Gasification Products From Coal and Refinery Residues,'' ASME paper 2000-GT-0026.
[5] Todd, D. M., and Battista, R. A., 2000, ''Demonstrated Applicability of Hydrogen Fuel for Gas Turbines,'' *Proc. of the IchemE Gasification 4 Conference*, Noordwijk, The Netherlands.
[6] Major, B., and Powers, B., 1999, ''Cost Analysis of NO_x Control Alternatives for Stationary Gas Turbines,'' Contract DE-Fc02-97CHIO877.
[7] Lozza, G., and Chiesa, P., 2002, ''Natural Gas Decarbonization to Reduce CO2 Emission From Combined Cycles. Part A: Partial Oxidation–Part B: Steam-Methane Reforming,'' ASME J. Eng. Gas Turbines Power, **124**(1), pp. 82–95.
[8] Andersen, T., Kvamsdal, H. M., and Bolland, O., 2000, ''Gas Turbine CC With CO_2 Capture Using Auto-Thermal Reforming of Natural Gas,'' ASME paper 2000-GT-0162.
[9] Louis, J. F., 1977, ''Systematic Studies of Heat Transfer and Film Cooling Effectiveness,'' in AGARD CP-229, Neuilly sur Seine, France.
[10] Chiesa, P., and Macchi, E., 2002, ''A Thermodynamic Analysis of Different Options to Break 60% Electric Efficiency in Combined Cycle Power Plants,'' ASME paper GT-2002-30663.
[11] Siemens Power Generation website: www.pg.siemens.com
[12] Heilos, A., Huth, M., Bonzani, F., and Pollarollo, G., 1998, ''Combustion of Refinery Residual Gas With a Siemens V94.2K Burner,'' Power Gen Europe, Milan, Italy.
[13] Huth, M., Vortmeyer, N., Schetter, B., and Karg, J., 1997, ''Gas Turbine Experience and Design for Syngas Operation,'' Gasification Technology in Practice, Institution of Chemical Engineers, Milan, Italy.
[14] Macchi, E., Consonni, S., Lozza, G., and Chiesa, P., 1995, ''An Assessment of the Thermodynamic Performance of Mixed Gas-Steam Cycles. Part A: Intercooled and Steam-Injected Cycles–Part B: Water-Injected and HAT Cycles,'' ASME J. Eng. Gas Turbines Power, **117**(3), pp. 489–498.